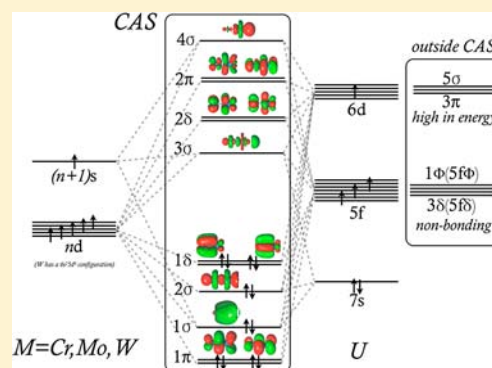


## Molecules with High Bond Orders and Ultrashort Bond Lengths: CrU, MoU, and WU

Fernando Ruipérez,<sup>†</sup> Gabriel Merino,<sup>‡</sup> Jesus M. Ugalde,<sup>†</sup> and Ivan Infante<sup>\*†</sup><sup>†</sup>Kimika Fakultatea, Euskal Herriko Unibertsitatea (UPV/EHU) and Donostia International Physics Center (DIPC), P. K. 20080 Donostia, Euskadi, Spain<sup>‡</sup>Departamento de Física Aplicada, Centro de Investigación y de Estudios Avanzados, 97310 Mérida, Yucatán, México

## Supporting Information

**ABSTRACT:** The structural and energetic parameters of MU hetero-bimetallic dimers (M = Cr, Mo, W) have been computed using the complete active space self-consistent-field method followed by second-order perturbation theory. Our results show that the effective bond order (EBO) of the MoU dimer (5.5) is higher than that for the tungsten dimer (5.2), known to date as the molecule with the highest EBO. These heterodimers present also ultrashort bond distances and remarkably large dissociation energies, which make these molecules suitable and interesting potential candidates in synthetic bimetallic organometallic chemistry.



## INTRODUCTION

In 1965, Cotton and co-workers showed strong evidence for the existence of an unprecedented quadruple bond between two rhenium atoms in the  $[\text{Re}_2\text{Cl}_8]^{2-}$  ion.<sup>1</sup> About 40 years later, Gagliardi and Roos found in silico<sup>2</sup> that the uranium dimer ( $\text{U}_2$ ) contains 10 bonding electrons to form a quintuple bond. Late in 2005, Power and co-workers reported the first synthesized quintuple bond between two metal atoms in the dichromium complex stabilized by bulky terphenyl ligands.<sup>3</sup> The authors suggested that two chromium(I) atoms share five electron pairs in five bonding orbitals, but given that the effective bond order (EBO) is less than 5, they preferred to use the term “fivefold bonding”. Since then, chemists have synthesized or proposed on paper many quintuple-bonded compounds.<sup>4–15</sup> Formally, the group VI atoms have six unpaired electrons in a  $nd^5(n+1)s^1$  electronic configuration (tungsten has a  $5d^46s^2$  configuration, but with a small  $s \rightarrow d$  promotion energy) that, in principle, allow them to form homonuclear dimers involving 12 bonding electrons, i.e., a sextuple bond. Specifically, the tungsten dimer ( $\text{W}_2$ ) has the strongest known sextuple bond, with an EBO<sup>5,6</sup> of 5.2.<sup>16</sup>

The additional shell of  $f$  atomic orbitals could, in principle, lead to higher bond multiplicities, but its contracted radial distribution prohibits this:<sup>5</sup> in the lanthanide series, the  $4f$  orbitals are too contracted to form any chemical bond; in the actinide series, the  $5f$  orbitals are more diffuse than the  $4f$  orbitals and can participate in bond formation but only from thorium to uranium. Beyond uranium, the  $5f$  orbitals become lanthanide-like and less prone to interact. The uranium atom has a  $5f^36d^17s^2$  ground-state electronic configuration, with a small  $s \rightarrow d$  promotion energy, which leads to six unpaired

electrons available to bond formation. As such,  $\text{U}_2$  is the only molecule that could be capable of reaching a bond multiplicity of 6.  $\text{U}_2$  has been computed with an equilibrium bond distance of 2.430 Å (see Table 1), in which the  $6d-6d$  and  $7s-7s$  orbital overlap is maximized, and only a little interaction between the  $5f$  orbitals is present.<sup>2</sup> This situation induces an unusual

**Table 1. Spectroscopic Constants of the CrU, MoU, and WU Dimers Computed at the CASSCF/CASPT2 Level of Theory<sup>a</sup>**

	$R_e$	$\Delta G_{1/2}$	CT	$k$	$D_e$	EBO	FSR
CrU	1.883	570	0.13	8.2	3.29 (3.88)	5.3	0.598
MoU	2.021	435	0.18	7.4	5.11 (6.14)	5.5	0.632
WU	2.080	353	0.19	7.6	4.14 (5.37)	5.3	0.671
$\text{Cr}_2^b$	1.679	452	0.0	3.1	1.53	4.5	0.600
$\text{Mo}_2^b$	1.938	477	0.0	6.2	4.41	5.2	0.668
$\text{W}_2^b$	2.010	337	0.0	6.2	5.37	5.2	0.744
$\text{U}_2^c$	2.430	265	0.0		1.20	4.2	0.694

<sup>a</sup>Bond distances (Å), vibrational frequencies ( $\Delta G_{1/2}$  in  $\text{cm}^{-1}$ ), force constants ( $k$  in  $\text{mdyn}/\text{Å}$ ), CT from uranium to metal (based on the Mulliken population), EBOs, and FSRs are all computed at the spin-free level; the dissociation energy ( $D_e$  in eV) is obtained at the RASSI-SO level of theory (spin-free values in parentheses), which includes spin-orbit coupling effects.  $D_e$  is computed by taking the energy difference between the total energy of the dimer at equilibrium and the sum of ground-state energies of the isolated atoms. <sup>b</sup>From ref 6. <sup>c</sup>From ref 2.

Received: July 31, 2012

Published: March 6, 2013

interaction that contains three electron-pair bonds, four one-electron bonds, and two ferromagnetic nonbonding electrons, for an EBO of 4.2, formally a quintuple bond.<sup>2</sup> A similar bonding situation is found in the chromium dimer ( $\text{Cr}_2$ ), whose atoms show a size imbalance for the valence 4s and 3d orbitals. The Cr–Cr potential energy surface (PES) shows a deep minimum at a short distance, 1.679 Å, corresponding to the most favorable overlap of the less diffuse 3d orbitals, while a shelf-like region at higher energies occurs when the 4s–4s interaction is dominant.<sup>17–20</sup>  $\text{Cr}_2$  has a strong multireference character and an EBO of only 4.5, despite the fact that it has the potential to develop a formal sextuple bond. Clearly, both  $\text{U}_2$  and  $\text{Cr}_2$  have EBOs much lower than that expected by pairing their 12 valence electrons. Two questions can immediately arise: (1) Can chromium and uranium form a heterobimetallic molecule with a bond stronger than those of their corresponding dimers? (2) Is there any heterobimetallic dimer with a bond order higher than that of  $\text{W}_2$ ?

## COMPUTATIONAL METHODOLOGY

It is well-known that in such types of systems there is a substantial mixing of configuration state functions (CSFs).<sup>2,16,19,21</sup> In view of that, we decided to employ the complete active space self-consistent-field (CASSCF) method,<sup>22–24</sup> followed by second-order perturbation (CASPT2) theory<sup>25,26</sup> for subsequent computation of the dynamic correlation energy. Scalar relativistic effects have been included using the Douglas–Kroll–Hess Hamiltonian,<sup>27,28</sup> while spin–orbit coupling has been added following the restricted active space state-interaction with spin–orbit coupling (RASSI-SO) method.<sup>29</sup> The basis set employed on each atom is the atomic natural orbital relativistic correlation consistent basis set of quadruple- $\zeta$  quality contracted to (10s9p7d5f3g2h) for uranium,<sup>30</sup> (7s5p4d3f2g) for chromium,<sup>31</sup> (8s7p5d3f2g) for molybdenum,<sup>31</sup> and (9s8p6d4f3g) for tungsten.<sup>31</sup>  $C_2$  symmetry has been imposed for all dimers. All computations have been done using the MOLCAS 7.4 package.<sup>32</sup>

A schematic view of the MU ( $M = \text{Cr}, \text{Mo}, \text{W}$ ) molecular orbital diagram is shown in Figure 1.

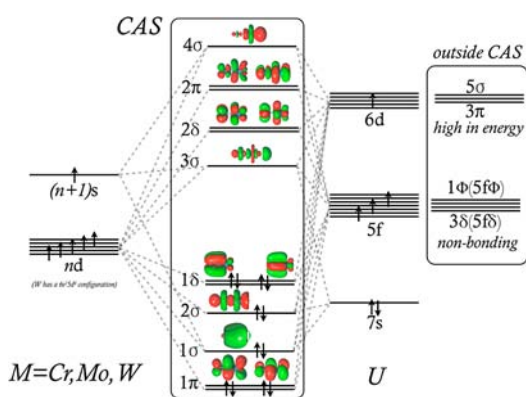


**Figure 1.** Schematic view of the bonding and antibonding orbital combinations included in the CAS between the group 6 transition-metal atoms  $M$  ( $M = \text{Cr}, \text{Mo}, \text{W}$ ) and uranium. Molecular orbitals not included in the CAS are also depicted. The plots are shown at the contour value of 0.02 e/bohr.<sup>3</sup>

The ideal active space would involve 12 electrons distributed in 19 orbitals [the thirteen 5f, 6d, and 7s orbitals of uranium and the six  $nd$  and  $(n + 1)s$  orbitals of the transition metal]. This space generates approximately  $1.5 \times 10^8$  CSFs and is too big for our computational resources. We decided then to follow a different approach by first analyzing a smaller active space and then increasing, step by step, its size. Clearly, our first option was to distribute 12 valence electrons in 12 molecular orbitals, that is, a (12/12) space. In this space, in

principle, the seven 5f orbitals were removed from the ideal (12/19) space. This choice, however, did not exclude the fact that inside the CAS the 5f orbitals mix with the 7s and 6d orbitals. Using the (12/12) active space, the ground state for the three MU dimers is a singlet  $^1\Sigma^+$ . To check whether this ground state was an artifact of the active space, we decided to test two larger active spaces where we added first the 5f orbitals, for a (12/14) space, and then the 5f $\phi$  orbitals, for a (12/16) space. These orbitals lie between the bonding/antibonding combinations and may yield a state with higher spin states or higher spin multiplicities with a more stable electronic structure. However, in both cases the same state  $^1\Sigma^+$  was found as the ground state. Three further orbitals, the doubly degenerate  $3\pi$  and  $5\sigma$  (Figure 1), could be included in the CAS but are usually found high in energy. On the basis of these considerations, the (12/12) active space was selected for further analysis. For consistency with previous papers, we have computed the bond order using the EBO scheme, which is particularly suitable for diatomic species.<sup>6</sup> The bond multiplicity is defined as the lowest integer value larger than the computed EBO.

## RESULTS AND DISCUSSION

The spin-free CASPT2 PES of the MU species are depicted in Figure 2. As anticipated, in the region near equilibrium, up until

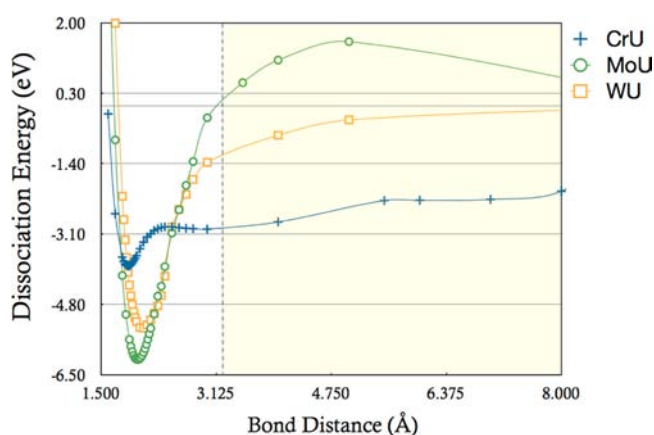


**Figure 2.** PES of the CrU, MoU, and WU dimers computed at the spin-free CASSCF/CASPT2 level of theory. The shaded part of the plot indicates the region where the CAS (12/12) is too small to correctly describe the PES.

3.0 Å, the CAS (12/12) provides a good approximation to the total wave function. Beyond this region, the CASSCF approximation most likely fails (shaded region in Figure 2) for two main reasons: (1) Along the dissociation of the M–U bond, the total wave function assumes a significant multi-reference character as the M–U molecular orbitals transform into orbitals mostly localized on the metal or uranium atoms. This means that a correct description of uranium would require seven extra orbitals, those that will be mostly localized in the 5f orbitals, which in the current (12/12) CAS approximation are taken out. (2) Despite its little reliability, the shaded part of the plot provides an important hint, i.e., that the energy curves of the singlet  $^1\Sigma^+$  ground state dissociate into an excited state. This is expected because the  $^1\Sigma^+$  state stems from the coupling of the metal and uranium atoms in their lowest septet states, which, in the case of chromium, for example, corresponds to the ground state but for uranium corresponds to an atomic excited state. This means that, at some point during the dissociation, a new state (or several) might overlap and then cross the  $^1\Sigma^+$  curve. The CASSCF approach, which is variational, will thus optimize the coefficients of this new state(s). While this might not be a problem, as we would just

follow the adiabatic energy curve, the energetic in this region is biased by the reasons explicated at point 1, and the zero energy reference at large separation would be wrong as a consequence of the limited CAS dimension.

In order for all MU dimers to share a common zero energy reference, we decided to sum up the ground-state CASSCF/CASPT2 energies of the corresponding isolated atoms as the reference energy. This can be obtained by computing the atoms separately in their most commonly employed CAS, i.e., (6/6) for the metal atoms and (6/13) for the uranium atom. This approach introduces an active-space imbalance at the CASSCF level because the CAS for the dimer, (12/12), does not add up to the one of the separated fragments, (6/6) + (6/13), which is virtually a (12/19) CAS. This imbalance is corrected, however, at the PT2 step, where also the semivalence electrons and all virtual orbitals are correlated. It has been demonstrated in a previous contribution<sup>20</sup> that this approach leads to a correct description of the dissociation limit and therefore of the dissociation energies. Moreover, because we chose the reference energy as the sum of the isolated atomic ground states, this explains why the MoU and WU energies quickly go toward zero as they are dissociating to an excited state. CrU behaves differently because it presents a shelf-like region at around 3 Å, as we will discuss later.

In summary, our approach provides reliable energy profiles in the region near equilibrium and accurate dissociation energies but fails to describe regions of the PES above 3 Å. From Figure 2, we have thus extracted the region around the minimum, in order to have a more detailed representation of the energy curves that we will use for the discussion (Figure 3).

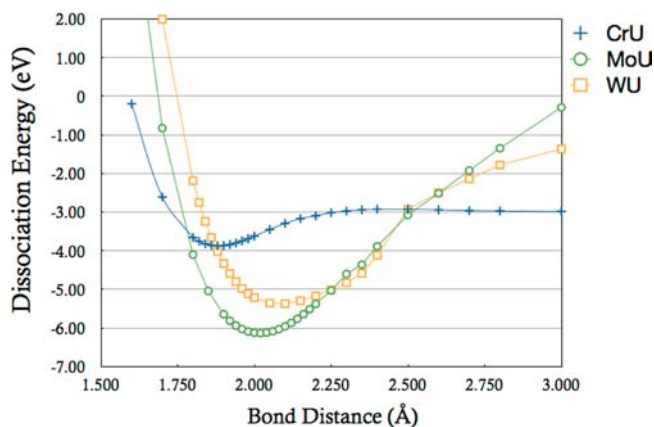


**Figure 3.** PES profiles around equilibrium of the CrU, MoU, and WU dimers computed at the spin-free CASSCF/CASPT2 level of theory.

The equilibrium bond lengths,  $R_e$ , are 1.883 (CrU), 2.021 (MoU), and 2.080 Å (WU), and the corresponding spin–orbit dissociation energies,  $D_e$ , are 3.29 (CrU), 5.11 (MoU), and 4.14 eV (WU). An increase of the reduced mass is accompanied by a decrease in the vibrational frequencies: 570 (CrU), 435 (MoU), and 353  $\text{cm}^{-1}$  (WU). These numbers are made clearer by a comparison with the homonuclear dimers. Table 1 summarizes the properties of both the MU and  $M_2$  dimers. Apparently, the  $D_e$  values of the MU are larger than those computed for  $M_2$ , except for WU. Interestingly, the deeper minima are found for MoU, and it is only around 0.2 eV smaller than the calculated value for  $W_2$  (5.37 eV).

In a heterodimer, the bond is not purely covalent. The difference in electronegativity between the two metals induces a

certain degree of ionicity, as opposed to homonuclear dimers. The consequence is that electrostatic effects could have an important role on the strength of the bond. Uranium (1.38, in the Pauling electronegativity scale) is less electronegative than chromium (1.66), molybdenum (2.16), and tungsten (2.36), so we expect an increase of the ionicity from CrU to WU. The charge transfer (CT) from uranium to the metal increases along the series. Inspection of Table 1 shows that this increase does not automatically turn into a stronger bond: the force constants follow an irregular trend where CrU has the largest value. In CrU, the size difference between the 4s and 3d orbitals on chromium and between the 5f orbitals and 6d and 7s orbitals on uranium leads to the formation of a minimum at short distances and a shelf-like potential at longer distances (see Figure 3, blue line). In this latter region, the bond is dominated mostly by the 4s–7s interaction. In molybdenum and tungsten, the size difference between the  $(n + 1)s$  and  $nd$  orbitals is mitigated by relativistic effects but does not disappear completely. As a consequence, MoU and WU present each one a single broad minimum. With the force constant being roughly inversely proportional to the width of the potential well, MoU and WU present computed force constants smaller than that of CrU, which has a sharper minimum at short distances. On the other hand, the spin–orbit coupling is usually much larger in the isolated atoms than in the molecule. Thus, the actual dissociation energies of the MU heterodimers are smaller upon inclusion of this term, with the largest effect seen for WU (see Table 1). The latter presents a spin–orbit  $D_e$  of 4.14 eV, 1.23 eV smaller than the spin-free value. In CrU, the spin–orbit coupling reduces the  $D_e$  value of only 0.59 eV, from 3.88 to 3.29 eV.

The total wave function of these MU species presents one dominant CSF, the closed-shell  $|1\sigma^2 2\sigma^2 1\pi^4 1\delta^4\rangle$ , which contributes approximately in a similar way for all complexes: 68% in CrU, 77% in MoU, and 69% in WU. Note that the same CSF in  $\text{Cr}_2$  contributes only 47% to the total wave function. In CrU, the increase of the contribution of this CSF is explained by the presence of a stronger bond than that in  $\text{Cr}_2$ . The stronger bonding interaction induces a larger separation from the antibonding component and, consequently, a reduction of the multiconfigurational mixing. The more diffuse 6d orbitals of uranium allow indeed for a better overlap with 3d orbitals than in the 3d–3d combination of  $\text{Cr}_2$ . The occupation number of the bonding 3d–6d orbitals in CrU is 3.66 (see Figure 4), much larger than that in  $\text{Cr}_2$  (3.16),<sup>6</sup> while the antibonding occupations are 0.34 and 0.84, respectively. In contrast to the homonuclear dimers, the 5f, 6d, and 7s orbitals can mix in the heterobimetallic species, enhancing the interaction with 3d, while 5f and 6d can both mix with 3d. For instance, in CrU, the 3d–5f/7s and 3d–5f/6d bonding orbitals have occupation numbers of 1.86 and 3.84, respectively, versus 1.77 and 3.62 found in  $\text{Cr}_2$  for 3d–3d and 3d–3d.

The synergy between 5f, 6d, and 7s orbitals promotes the formation of very short MU bonds with large EBOs. For example, it is striking that the CrU has a bond length 0.6 Å shorter than that in  $\text{U}_2$  and only 0.1 Å larger than that in  $\text{Cr}_2$ . To have an idea of how short this bond actually is, we can make use of the formal shortness ratio (FSR), defined by Cotton,<sup>33</sup> a parameter computed as the ratio between the A–B bond distance and the sum of the A and B radii. While the atomic radius definition of an atom remains somewhat arbitrary, the FSR has been successfully used to identify unusually short metal–metal bond distances in newly synthesized compounds.

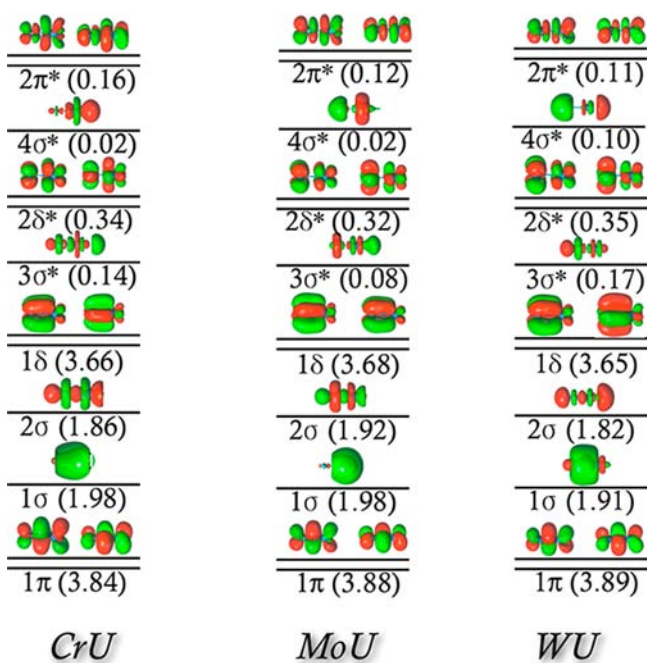


**Figure 4.** Bonding and antibonding natural orbitals computed at the spin-free CASSCF level of theory for all MU species. The natural occupation numbers are given in parentheses below each natural orbital. The plots are depicted at the contour value of 0.02 e/bohr.<sup>3</sup>

For instance, the shortest homobimetallic bond ever found in an organometallic complex involves two chromium atoms, with a bond distance of 1.75 Å,<sup>34–37</sup> only 0.06 Å larger than the gas-phase Cr<sub>2</sub> value. Assuming a chromium radius of 1.40 Å (from the empirical Slater radii<sup>38</sup>), their FSRs are 0.625 and 0.600, respectively. Using these values as reference for the definition of a very short, or ultrashort, bond, we determined the FSRs for the heterobimetallic dimers computed in this work (see Table 1). For the radii of Mo, W, and U, we used 1.45, 1.35, and 1.75 Å, respectively. CrU has a FSR of 0.598, even smaller than that of Cr<sub>2</sub>, indicating in this way the remarkable shortness of this bond length. It is also interesting that all of the other heterodimers have a FSR smaller than those of their corresponding homonuclear dimers. This surprisingly short bond distances are very likely connected to the high bond order of these molecules. For example, the EBO of CrU is 5.3, that is, a sextuple bond. This is the only molecule in the literature containing the chromium atom that can reach such a high bond order and, consequently, a large dissociation energy. The only two heterobimetallic molecules that can challenge this EBO are CrMo and CrW, but they have been shown to be 4.7 and 4.4, respectively,<sup>39</sup> still lower than that of CrU. The same enhancing effect on the EBO is also noted for MoU (5.5) and WU (5.3), which have EBOs higher than those of their homonuclear counterparts. In particular, MoU shows the highest bond order of any given metal–metal combination in the whole periodic table.

This enhanced effect on the EBO is more intense for the CrU molecule, which changes from 4.5 in Cr<sub>2</sub> to 5.3. In MoU and WU, the EBOs increase by only 0.3 and 0.1, respectively. As explained earlier, this enhancement is induced by the synergic effect of the 5f orbitals, which have a positive effect in strengthening the bond, in particular for CrU.

A further point of interest in these species is the presence of multiple  $\sigma$  bonds. The concept of double  $\sigma$  bonds has in recent

years gained momentum because it has allowed speculation about the presence of a quadruple bond in C<sub>2</sub><sup>43</sup> or in more exotic species like CUO.<sup>44</sup> Basically, thanks to the closeness in the radial extension of the 2s and 2p orbitals, the carbon atom can generate two  $\sigma$  sp hybrid orbitals (top left of Figure 5). In

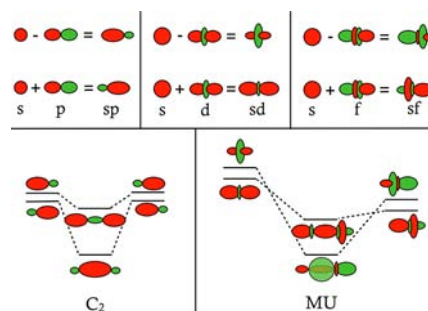


**Figure 5.** (Top) Generic sp, sd, and sf hybrid orbitals. (Bottom) Schematic representation of the double  $\sigma$  bond in the MU heterodimers. The C<sub>2</sub> molecular orbital diagram is shown for comparison.

C<sub>2</sub>, these hybrid orbitals interact to form one  $\sigma$  bond by overlapping the two larger lobes and one weak “rearward” bond, with the latter stemming from an overlap between the smaller lobes of the sp tail (bottom left of Figure 5). Inspection of Table 2 shows that the doubly occupied  $\sigma$ -bonding orbitals 1 $\sigma$  and 2 $\sigma$  in the MU heterodimers are composed mostly of s and d orbitals localized on the transition metal atom M and of 7s and 5f on uranium. In the latter, the 6d orbital is higher in energy; therefore, for the sake of simplicity, we will not discuss its contribution to the bond. The transition metal M  $\sigma$ -types of orbitals can be represented in terms of sd hybridization, with one sd orbital shaped by two big axial lobes with the same sign and a small equatorial ring with the opposite sign and another sd orbital with two smaller axial lobes and a much more diffuse equatorial ring (top middle of Figure 5). On the other hand, the sf (7s–5f) hybridization of uranium leads to two specular orbitals identified by one bigger and one smaller axial lobes of different sign and one bigger and one smaller equatorial rings also with opposite sign (top right of Figure 5). Interestingly, when M and uranium interact, two types of  $\sigma$  bonding are obtained (bottom right of Figure 5): (a) the former, more stable, can be described as a bond where both the more diffuse ring and the smaller lobe on the sf hybrid orbital synergically combine in-phase with the smaller lobe and the diffuse ring of the sd hybrid orbital on M; (b) the second  $\sigma$  bond, less stable, is mostly defined by the overlap of the two main bigger lobes on the sd and sf hybrid orbitals. While this second bond is constructed in the same fashion as the sp–sp main  $\sigma$  frontward bond in C<sub>2</sub>, the former can be seen as having a dual nature, in which we can extract a rearward bond, in which the main axial lobes interact with the smaller sd and sf lobes, but also a frontward bond, where the very diffuse equatorial rings of sd and sf hybrid orbitals overlap with each other.

## CONCLUSIONS

In this paper, we analyzed the structural and energetic properties of MU heterobimetallic dimers (M = Cr, Mo, W) based on calculations performed at the CASSCF/CASPT2 level of theory. Our main result shows that the EBO of MoU is higher than that for W<sub>2</sub>, which has been considered so far as the molecule with the highest bond order. Another important

Table 2. Composition of the 1 $\sigma$  and 2 $\sigma$  Molecular Orbitals Computed at the CASSCF/CASPT2 Level of Theory

	CrU		MoU		WU	
	Cr (%)	U (%)	Mo (%)	U (%)	W (%)	U (%)
1 $\sigma$	3d $\sigma$ (32) + 4s $\sigma$ (11)	7s $\sigma$ (31) + 5f $\sigma$ (18)	4d $\sigma$ (35) + 4s $\sigma$ (10)	7s $\sigma$ (28) + 5f $\sigma$ (22)	6s $\sigma$ (28) + 5d $\sigma$ (12)	7s $\sigma$ (42) + 5f $\sigma$ (10)
2 $\sigma$	3d $\sigma$ (17) + 4s $\sigma$ (9)	7s $\sigma$ (50) + 5f $\sigma$ (16)	5s $\sigma$ (35) + 4d $\sigma$ (15)	7s $\sigma$ (25) + 5f $\sigma$ (11)	5d $\sigma$ (31) + 6s $\sigma$ (17)	5f $\sigma$ (21) + 7s $\sigma$ (10)

consequence of this work is the possibility of using the computed spectroscopic parameters as reference for future experimental works in novel exotic species. In the last decades, metal–metal bond chemistry has been the subject of a huge amount of research that helped to go beyond the current view. However, some aspects have not been clarified yet, and we hereby summarize (a) metal–metal bonding in the f-block chemistry is scarcely known,<sup>40,41</sup> (b) transition-metal hetero-bimetallic metal–metal bonds face synthetic challenges and are also rather scarce,<sup>42</sup> and (c) the successful synthetic attempts for very short Cr–Cr bonds turned out to be a consequence of a strain effect of the ligands rather than an efficient overlap between the chromium orbitals. In this sense, our results provide some important clues on aspects a and c. The predicted large dissociation energies indicate a remarkable chemical affinity between uranium and group VI elements. Certainly, this could help to overcome one of the central problems in the synthesis of complexes with metal–metal bonds in the f block, that is, the weak interactions between the two metal centers. Moreover, the sextuple bond in Cr–U can be envisaged as a target for the synthesis of molecules containing ultrashort bimetallic bonds, bearing an effective covalent interaction between the two metal atoms.

## ■ ASSOCIATED CONTENT

### 📄 Supporting Information

CASSCF and CASPT2 total energies, along with a figure of their energy profiles. This material is available free of charge via the Internet at <http://pubs.acs.org>.

## ■ AUTHOR INFORMATION

### Corresponding Author

\*E-mail: [iinfant76@gmail.com](mailto:iinfant76@gmail.com).

### Author Contributions

The manuscript was written through contributions of all authors. All authors have given approval to the final version of the manuscript.

### Notes

The authors declare no competing financial interest.

## ■ ACKNOWLEDGMENTS

Financial support comes from Eusko Jaurlaritza (Grant GIC 07/85 IT-330-07) and the Spanish Office for Scientific Research (Grant CTQ2011-27374). The SGI/IZO-SGIker UPV/EHU is gratefully acknowledged for generous allocation of computational resources. G.M. gratefully acknowledges support from Ikerbasque.

## ■ REFERENCES

- (1) Cotton, F. A.; Harris, C. B. *Inorg. Chem.* **1965**, *4*, 330.
- (2) Gagliardi, L.; Roos, B. O. *Nature* **2005**, *433*, 848.
- (3) Nguyen, T.; Sutton, A. D.; Brynda, M.; Fetting, J. C.; Long, G. J.; Power, P. P. *Science* **2005**, *310*, 844.
- (4) Chisholm, M. H.; Macintosh, A. M. *Chem. Rev.* **2005**, *105*, 2949.
- (5) Roos, B. O.; Malmqvist, P.-Å.; Gagliardi, L. *J. Am. Chem. Soc.* **2006**, *128*, 17000.

- (6) Roos, B. O.; Borin, A. C.; Gagliardi, L. *Angew. Chem., Int. Ed.* **2007**, *46*, 1469.
- (7) Frenking, G. *Science* **2005**, *310*, 796.
- (8) Landis, C. R.; Weinhold, F. *J. Am. Chem. Soc.* **2006**, *128*, 7335.
- (9) Merino, G.; Donald, K. J.; D'Acchioli, J. S.; Hoffmann, R. *J. Am. Chem. Soc.* **2007**, *129*, 15295.
- (10) Brynda, M.; Gagliardi, L.; Widmark, P. O.; Power, P. P.; Roos, B. O. *Angew. Chem., Int. Ed.* **2006**, *45*, 3804.
- (11) Weinhold, F.; Landis, C. R. *Science* **2007**, *316*, 61.
- (12) Li Manni, G.; Dzubak, A. L.; Mulla, A.; Brogden, D. W.; Berry, J. F.; Gagliardi, L. *Chem.—Eur. J.* **2012**, *18*, 1737.
- (13) La Macchia, G.; Gagliardi, L.; Power, P. P.; Brynda, M. *J. Am. Chem. Soc.* **2008**, *130*, 5104.
- (14) La Macchia, G.; Li Manni, G.; Todorova, T. K.; Brynda, M.; Aquilante, F.; Roos, B. O.; Gagliardi, L. *Inorg. Chem.* **2010**, *49*, 5216.
- (15) Brynda, M.; Gagliardi, L.; Roos, B. O. *Chem. Phys. Lett.* **2009**, *471*, 1.
- (16) Borin, A. C.; Gobbo, J. P.; Roos, B. O. *Chem. Phys. Lett.* **2010**, *490*, 24.
- (17) Casey, S. M.; Leopold, D. G. *J. Phys. Chem.* **1993**, *97*, 816.
- (18) Andersson, K.; Roos, B. O.; Malmqvist, P.-Å.; Widmark, P.-O. *Chem. Phys. Lett.* **1994**, *230*, 391.
- (19) Roos, B. O. *Collect. Czech. Chem. Commun.* **2003**, *68*, 265.
- (20) Ruipérez, F.; Aquilante, F.; Ugalde, J. M.; Infante, I. *J. Chem. Theory Comput.* **2011**, *7*, 1640.
- (21) Borin, A. C.; Gobbo, J. P.; Roos, B. O. *Chem. Phys.* **2008**, *343*, 210.
- (22) Roos, B. O.; Taylor, P. R.; Siegbahn, P. E. M. *Chem. Phys.* **1980**, *48*, 157.
- (23) Siegbahn, P. E. M.; Heiberg, A.; Roos, B. O.; Levy, B. *Phys. Scr.* **1980**, *21*, 323.
- (24) Siegbahn, P. E. M.; Heiberg, A.; Almlöf, J.; Roos, B. O. *J. Chem. Phys.* **1981**, *74*, 2384.
- (25) Andersson, K.; Malmqvist, P.-Å.; Roos, B. O.; Sadlej, A. J.; Wolinski, K. *J. Phys. Chem.* **1990**, *94*, 5483.
- (26) Andersson, K.; Malmqvist, P.-Å.; Roos, B. O. *J. Chem. Phys.* **1992**, *96*, 1218.
- (27) Douglas, M.; Kroll, N. M. *Ann. Phys. (N.Y.)* **1974**, *82*, 89.
- (28) Hess, B. A. *Phys. Rev. A* **1986**, *33*, 3742.
- (29) Malmqvist, P.-Å.; Roos, B. O.; Schimmelpennig, B. *Chem. Phys. Lett.* **2002**, *357*, 230.
- (30) Roos, B. O.; Lindh, R.; Malmqvist, P.-Å.; Veryazov, V.; Widmark, P.-O. *Chem. Phys. Lett.* **2005**, *409*, 295.
- (31) Roos, B. O.; Lindh, R.; Malmqvist, P.-Å.; Veryazov, V.; Widmark, P.-O. *J. Phys. Chem. A* **2005**, *109*, 6575.
- (32) Aquilante, F.; De Vico, L.; Ferré, N.; Ghigo, G.; Malmqvist, P.-Å.; Neogrády, P.; Pedersen, T. B.; Pitoňák, M.; Reiher, M.; Roos, B. O.; Serrano-Andrés, L.; Urban, M.; Veryazov, V.; Lindh, R. *J. Comput. Chem.* **2010**, *31*, 224.
- (33) Cotton, F. A. *Acc. Chem. Res.* **1978**, *11*, 225.
- (34) Tsai, Y.-C.; Hsu, C.-W.; Yu, J.-S. K.; Lee, G.-H.; Wang, Y.; Kuo, T.-S. *Angew. Chem., Int. Ed.* **2008**, *47*, 7250.
- (35) Noor, A.; Wagner, F. R.; Kempe, R. *Angew. Chem., Int. Ed.* **2008**, *47*, 7246.
- (36) Hsu, C.-W.; Yu, J.-S. K.; Yen, C.-H.; Lee, G.-H.; Wang, Y.; Tsai, Y.-C. *Angew. Chem., Int. Ed.* **2008**, *47*, 9933.
- (37) Wagner, F. R.; Noor, A.; Kempe, R. *Nat. Chem.* **2009**, *1*, 529.
- (38) Slater, J. C. *J. Chem. Phys.* **1964**, *41*, 3199.
- (39) Ruipérez, F.; Ugalde, J. M.; Infante, I. *Inorg. Chem.* **2011**, *50*, 9219.
- (40) Liddle, S. T.; Mills, D. P. *Dalton Trans.* **2009**, 5592.

(41) Oelkers, B.; Butovskii, M. V.; Kempe, R. *Chem.—Eur. J.* **2012**, *18*, 13566.

(42) Vlasisavljevich, B.; Miró, P.; Cramer, C. J.; Gagliardi, L.; Infante, I.; Liddle, S. T. *Chem.—Eur. J.* **2011**, *17*, 8424.

(43) Shaik, S.; Danovich, D.; Wu, W.; Su, P.; Rzepa, H. S.; Hiberty, P. C. *Nat. Chem.* **2012**, *4*, 195.

(44) Hu, H.; Qui, Y.; Xiong, X.; Schwarz, W. H. E.; Li, J. *Chem. Sci.* **2012**, *3*, 2786.